

Glucose and glutamine metabolism-related protein expression in breast ductal carcinoma *in situ*

Hyang Joo RYU, Ja Seung KOO*

Department of Pathology, Yonsei University College of Medicine, Seoul, South Korea

*Correspondence: kjs1976@yuhs.ac

Received January 3, 2022 / Accepted March 1, 2022

Glucose and glutamine metabolism is involved in important tumor mechanisms. Metabolism-related protein expression has been previously reported to predict tumor prognosis. We aimed to investigate glucose and glutamine metabolism-related protein expression and its implication in breast ductal carcinoma *in situ* (DCIS). A tissue microarray was prepared for 205 DCIS cases. Glucose and glutamine metabolism-related proteins were immunostained. Based on the results of estrogen receptor, progesterone receptor, human epidermal growth factor receptor (HER)-2, and Ki-67, DCIS was classified into the luminal type, HER-2 type, and triple-negative breast cancer (TNBC). DCIS stroma was classified into non-inflammatory and inflammatory types per stromal histology. DCIS (N=205) was classified into luminal type (n=112), HER-2 type (n=81), and TNBC (n=12). Hexokinase II (p=0.044), GLS (p=0.003), and SLC7A5 (p<0.001) expression rates were the highest in TNBC. Inflammatory type stroma showed higher SLC7A5 (p<0.001) and SLC7A11 (p=0.008) expression rates than non-inflammatory type stroma. In summary, DCIS demonstrated differential expression of metabolism-related proteins according to the molecular subtype and stromal features. TNBC showed the highest glucose and glutamine metabolism-related protein expression, and inflammatory type stroma showed higher glutamine metabolism-related protein expression than non-inflammatory type stroma.

Key words: breast; ductal carcinoma in situ; metabolism; glucose; glutamine

Ductal carcinoma *in situ* (DCIS) is the pre-invasive lesion of invasive breast cancer. It is well known that breast cancer develops from normal epithelium through atypical ductal hyperplasia (ADH), and DCIS finally develops into invasive cancer. Therefore, DCIS is the direct precursor of invasive breast cancer, and this has been supported by previous findings that about 50% of invasive carcinomas are accompanied by DCIS [1] and the genetic features among ADH, DCIS, and invasive carcinoma overlap significantly [2]. However, the finding that only 20–50% of DCIS cases progress into invasive carcinoma, even when no treatment is applied, suggests that additional events are required for the progression of DCIS into invasive carcinoma [3–5].

The metabolic shift from oxidative phosphorylation to anaerobic glycolysis, also known as the Warburg effect, is the metabolic characteristic of cancer cells [6, 7]. The important molecules involved in glycolysis include glucose transporter (GLUT)-1, hexokinase II, and carbonic anhydrase (CA) IX. GLUT-1 transports glucose into the cell [8], and hexokinase II is the enzyme that phosphorylates intracellular glucose into glucose-6-phosphate [9]. CA IX neutralizes the

acidity caused by lactate formed during glycolysis via reversible hydration of carbon dioxide [10]. Another important element of tumor metabolism is glutamine metabolism. The importance of glutamine metabolism in the cancer cell lies in ensuring that two important factors, i.e., ATP production and intermediate supply for macromolecular synthesis, occur in the proliferating tumor cell [11]. The important proteins in glutamine metabolism include glutaminase 1 (GLS1) [12], an enzyme that converts glutamine into glutamate, and membrane-bound solution carrier (SLC) transporter, an amino acid transporter. Previous studies have reported the differences in metabolic phenotypes depending on the tumor subtype [13–15], and some have further reported that metabolism-related protein expression can predict cancer prognosis [16–18].

There have been many studies demonstrating the importance of glucose/glutamine metabolism in several invasive carcinomas [19, 20]. In the breast, invasive ductal carcinoma has been actively researched. Breast carcinoma is known to be progressed carcinoma, and there is a preceding lesion called DCIS before invasive ductal carcinoma. DCIS is a histo-

logically heterogeneous non-obligate precursor of invasive breast carcinoma, and the molecular subtype including high nuclear grade is known to be a risk factor for progression of DCIS to invasive carcinoma [21]. However, studies about glucose/glutamine metabolism on DCIS, an independent entity, are insufficient. Moreover, studies on the characteristics of these metabolisms and molecular subtypes in DCIS are also lacking.

The purpose of this study was to compare and investigate glucose and glutamine metabolism-related protein expression and its clinical implication in breast DCIS.

Patients and methods

Patient selection and histological evaluation. Patients diagnosed with DCIS and operated at Severance Hospital from January 2000 to December 2006 were included in this study. Patients who received chemotherapy or hormonal therapy before surgery were excluded. This study was approved by the Institutional Review Board (IRB) of Yonsei University Severance Hospital. The IRB waived the requirement to obtain informed consent from patients. The study conforms to The Code of Ethics of the World Medical Association (Declaration of Helsinki). All the cases were reviewed by the breast pathologist (Koo JS) using Hematoxylin & Eosin (H&E)-stained slides. Histological grade was assessed using the Nottingham grading system [22]. Clinicopathological parameters evaluated in each case included patient age at initial diagnosis, lymph node metastasis, tumor recurrence, distant metastasis, and patient survival.

DCIS stroma was microscopically observed and classified into inflammatory (the tumor stroma is mainly composed of inflammatory cells, such as lymphocytes) and non-inflammatory (the tumor stroma is not mainly configured by inflammatory cells) types.

Tissue microarray. A representative area showing the tumor and tumor stroma was selected on an H&E-stained slide, and a corresponding spot was marked on the surface of the paraffin block. Using a biopsy needle, the selected area was punched out, and a 3 mm tissue core was transferred to a 6×5 recipient block. Two tissue cores of invasive tumor were extracted to minimize extraction bias. Each tissue core was assigned a unique tissue microarray location number that was linked to a database containing other clinicopathological data.

Immunohistochemistry. Immunohistochemistry was performed for formalin-fixed, paraffin-embedded tissue sections and with BenchMark automated staining instrument (Ventana Medical System, Tucson, AZ, USA). Primary antibodies used for immunohistochemistry are listed in Supplementary Table S1. Briefly, tissue sections were sectioned to 5 μm thickness, deparaffinized in xylene, rehydrated in three graded alcohol chambers, and treated with 3% hydrogen peroxide in methanol. For visualization of staining, a DAB detection kit (Ventana Medical Systems)

was used. The primary antibody incubation step was omitted for the negative control. Staining of the positive control tissue was performed according to the manufacturer's instructions (hexokinase II: thyroid tumor, GLUT1, CA IX, SLC7A5: esophageal carcinoma, GLS, ASCT2: colon, SLC7A11: small bowel).

Interpretation of immunohistochemical staining. All immunohistochemical markers were assessed by light microscopy. A cut-off value of ≥1% positively stained nuclei was used to define estrogen receptor (ER), progesterone receptor (PR), and androgen receptor positivity [23]. Human epidermal growth factor receptor (HER)-2-stained tissues were analyzed according to the American Society of Clinical Oncology (ASCO)/College of American Pathologists (CAP) guidelines, as follows: 0 = no immunostaining; 1+ = weak incomplete membranous staining, <10% of tumor cells; 2+ = complete membranous staining, either uniform or weak in ≥10% of tumor cells; and 3+ = uniform intense membranous staining in ≥30% of tumor cells [24]. HER-2 immunostaining was considered positive when strong (3+) membranous staining was observed and negative when no or weak (0 to 1+) membranous staining was observed. Immunohistochemistry of glucose/glutamine metabolism-related protein expression was analyzed using the semi-quantitative H-score method. The method yielded a total score range of 0 to 300 by multiplying the dominant staining intensity score (0, no staining; 1, weak or barely detectable staining; 2, distinct brown staining; 3, strong dark brown staining) by the percentage (0–100%) of positive cells. The sample was divided into three groups (negative, low expression, high expression), and the cut-off value was calculated for the mean value of protein expression.

Tumor phenotype classification. In this study, we classified breast cancer phenotypes according to the immunohistochemistry results for ER, PR, HER-2, and Ki-67 and FISH results for HER-2, as follows: *luminal A type*- ER or/and PR positive, HER-2 negative, and Ki-67 labeling index (LI) <14%; *luminal B type* (HER-2 negative)- ER or/and PR positive, HER-2 negative, and Ki-67 LI ≥14%; *luminal B type* (HER-2 positive)- ER or/and PR positive and HER-2 overexpressed or/and amplified; *HER-2 overexpression type*- ER and PR negative and HER-2 overexpressed or/and amplified; *TNBC type*- ER, PR, and HER-2 negative [25].

Statistical analysis. Data were analyzed using SPSS for Windows, Version 25.0 (SPSS Inc., Chicago, IL, USA). For determination of significance, Student's *t* and Fisher's exact tests were used for continuous and categorical variables, respectively. Significance was set at *p*<0.05. Kaplan-Meier survival curves and log-rank statistics were employed to evaluate time to tumor recurrence and overall survival.

Results

Basal characteristics of patients with DCIS. The basic characteristics of 205 patients with DCIS included in this

study are presented in Supplementary Table S2. DCIS (N=205) was classified into luminal type (n=112), HER-2 type (n=81), and TNBC (n=12). Significant differences in the age (p=0.047), architecture type (p=0.002), nuclear grade (p=0.002), necrosis (p<0.001), and stromal type (p<0.001) were observed according to the molecular subtype. The rates of comedo-type necrosis and inflammatory type stroma were significantly higher in HER-2 type and TNBC than in other subtypes, and the rate of the high nuclear grade was significantly higher in TNBC than in other subtypes (p<0.001).

Metabolism-related protein expression in DCIS according to the molecular subtypes. First, we investigated glucose metabolism-related protein expression in DCIS according to the molecular subtype and observed significant differences in hexokinase II (p=0.044) expression among different molecular subtypes, with the lowest negative rate observed in TNBC (Table 1 and Figure 1). Two types of GLUT-1 expression patterns were observed. The first expression pattern was observed throughout the tumor without a specific zonal pattern, and the second expression pattern

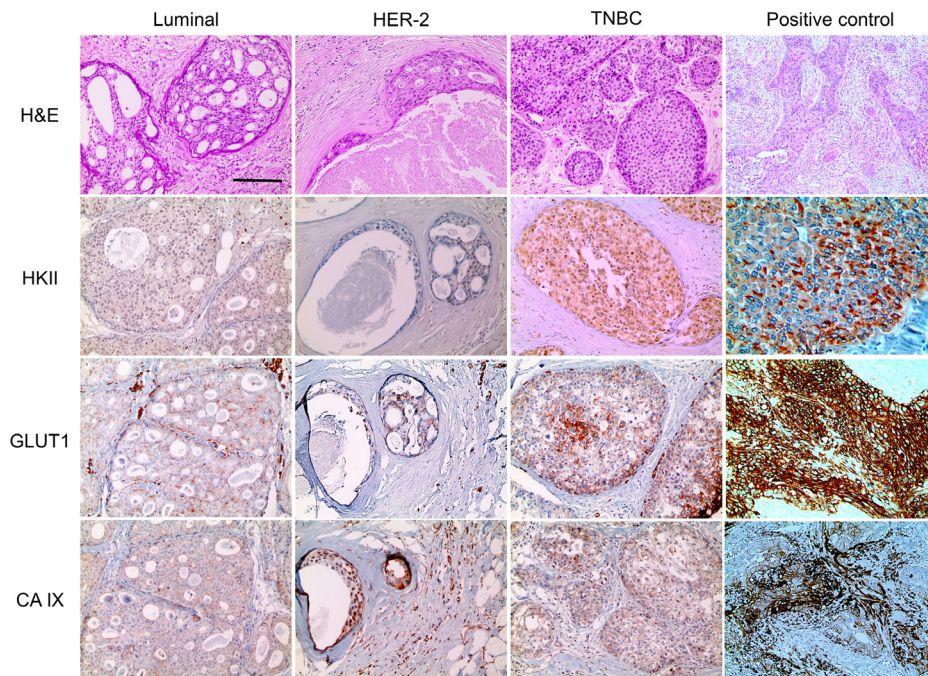


Figure 1. Glucose metabolism-related protein expression in ductal carcinoma in situ (DCIS) according to the molecular subtypes. Hexokinase II expression was higher in triple-negative breast cancer (TNBC) than in other subtypes. Positive control tissues were as follows; hexokinase II: thyroid tumor, GLUT1, CA IX: esophageal carcinoma. Scale bar = 500 μ m

Table 1. Glucose metabolism-related protein expression in ductal carcinoma in situ according to molecular subtype.

Parameters	Total N=205 (%)	Molecular subtype			p-value
		Luminal n=112 (%)	HER-2 n=81 (%)	TNBC n=12 (%)	
Hexokinase II					0.044
Negative	188 (91.7)	99 (88.4)	79 (97.5)	10 (83.3)	
Low expression	11 (4.5)	7 (6.2)	2 (2.5)	2 (16.7)	
High expression	6 (3.8)	6 (5.4)	0 (0.0)	0 (0.0)	
GLUT 1					0.179
Negative	107 (52.2)	55 (49.1)	47 (58.0)	5 (41.7)	
Low expression	67 (32.7)	38 (33.9)	22 (27.2)	7 (58.3)	
High expression	31 (15.1)	19 (17.0)	12 (14.8)	0 (0.0)	
CA IX					0.111
Negative	59 (28.8)	33 (29.5)	25 (30.9)	1 (8.3)	
Low expression	71 (34.6)	44 (39.3)	24 (29.6)	3 (25.0)	
High expression	75 (36.6)	35 (31.2)	32 (39.5)	8 (66.7)	

Abbreviations: TNBC-triple-negative breast cancer; CA-carbonic anhydrase

appeared to be focused in the central zone. The latter expression pattern was often observed around the comedo-type central necrosis (Figure 2).

Next, we investigated glutamine metabolism-related protein expression in DCIS according to the molecular subtype and observed significant differences in GLS ($p=0.003$) and SLC7A5 ($p<0.001$) among the different molecular subtypes, with the highest expression observed in TNBC (Table 2 and Figure 3). There was no statistically significant difference between the expression results of hexokinase II and GLS/SLC7A5, which showed a significant difference in expression rate according to molecular subtypes ($p=0.902$ and $p=0.336$, respectively, Supplementary Table S3).

Metabolism-related protein expression in DCIS according to the stromal subtypes. No significant difference in glucose metabolism-related protein expression in DCIS was observed according to the stromal subtypes (Table 3). However, significant differences in glutamine metabolism-related protein expression were observed depending on the stromal subtypes, with higher SLC7A5 ($p<0.001$) and SLC7A11 ($p=0.008$) expression rates in the inflammatory type stroma than in the non-inflammatory type stroma (Table 4).

Correlation between the clinicopathological factors and metabolism-related protein expression. During investigating the association between metabolism-related protein

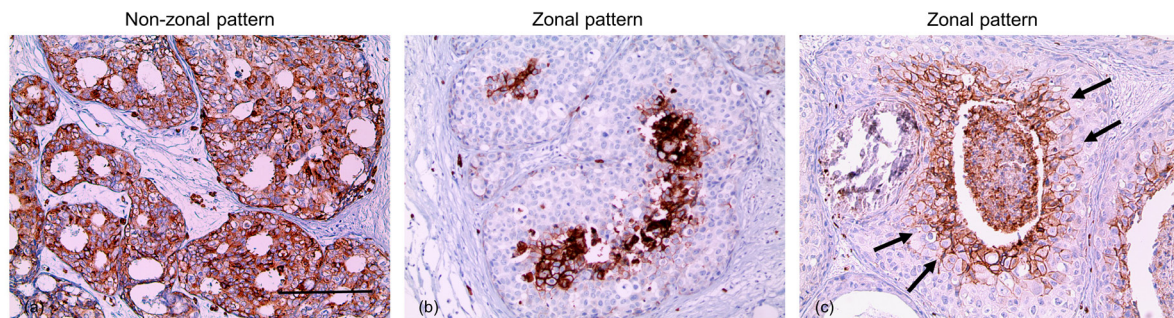


Figure 2. Glucose transporter (GLUT)-1 expression patterns in DCIS. Two types of GLUT-1 expression patterns were observed. The first expression pattern was observed throughout the tumor without a specific zonal pattern (a), and the second expression pattern appeared to be focused in the central zone (b, c). The latter expression pattern was particularly evident around the comedo-type necrosis (c, arrow). Scale bar = 500 μm

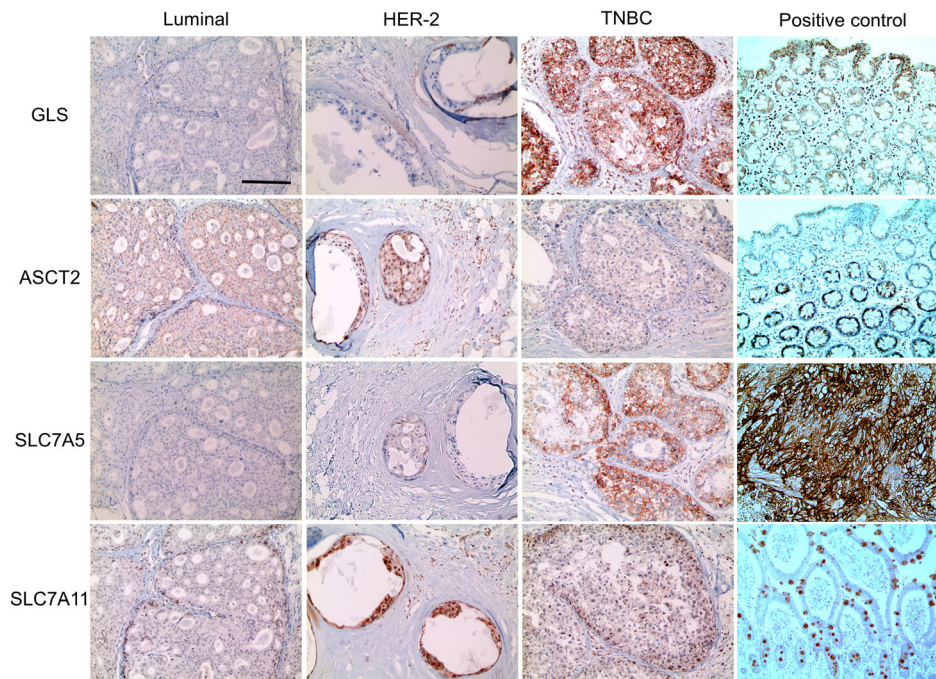


Figure 3. Glutamine metabolism-related protein expression in DCIS according to the molecular subtypes. GLS and SLC7A5 expressions were higher in triple-negative breast cancer than in other subtypes. Positive control tissues were as follows; SLC7A5: esophageal carcinoma, GLS, ASCT2: colon, SLC7A11: small bowel. Scale bar = 500 μm

Table 2. Glutamine metabolism-related protein expression in ductal carcinoma in situ according to molecular subtype.

Parameters	Total N=205 (%)	Molecular subtype			p-value
		Luminal n=112 (%)	HER-2 n=81 (%)	TNBC n=12 (%)	
GLS					0.003
Negative	171 (83.4)	100 (89.3)	65 (80.2)	6 (50.0)	
Low expression	22 (10.7)	7 (6.2)	12 (14.8)	3 (25.0)	
High expression	12 (5.9)	5 (4.5)	4 (4.9)	3 (25.0)	
ASCT2					0.377
Negative	127 (62.0)	69 (61.6)	52 (64.2)	6 (50.0)	
Low expression	53 (25.9)	27 (24.1)	23 (28.4)	3 (25.0)	
High expression	25 (12.1)	16 (14.3)	6 (7.4)	3 (25.0)	
SLC7A5					< 0.001
Negative	183 (89.3)	105 (93.8)	72 (88.9)	6 (50.0)	
Low expression	12 (5.8)	4 (3.6)	5 (6.2)	3 (25.0)	
High expression	10 (4.9)	3 (2.7)	4 (4.9)	3 (25.0)	
SLC7A11					0.284
Negative	181 (88.4)	102 (91.1)	69 (85.2)	10 (83.3)	
Low expression	12 (5.8)	4 (3.6)	6 (7.4)	2 (16.7)	
High expression	12 (5.8)	6 (5.4)	6 (7.4)	0 (0)	

Abbreviations: TNBC-triple-negative breast cancer; GLS-glutaminase; ASCT-amino acid transporter; SLC-membrane-bound solution carrier

Table 3. Glucose metabolism-related protein expression in ductal carcinoma in situ according to stromal type.

Parameters	Total N=205 (%)	Stromal type		p-value
		Non-inflammatory n=153 (%)	Inflammatory n=52 (%)	
Hexokinase II				0.876
Negative	188 (91.7)	140 (91.5)	48 (92.3)	
Low expression	11 (5.4)	8 (5.2)	3 (5.8)	
High expression	6 (2.9)	5 (3.3)	1 (1.9)	
GLUT 1				0.683
Negative	107 (52.2)	78 (51.0)	29 (55.8)	
Low expression	67 (32.7)	50 (32.7)	17 (32.7)	
High expression	31 (15.1)	25 (16.3)	6 (11.5)	
CA IX				0.121
Negative	59 (28.8)	48 (31.4)	11 (21.2)	
Low expression	71 (34.6)	55 (35.9)	16 (30.8)	
High expression	75 (36.6)	50 (32.7)	25 (48.1)	

Abbreviations: GLUT-glucose transporter; CA-carbonic anhydrase

expression and the clinicopathological factors in DCIS, we found that DCIS necrosis was significantly associated with GLUT-1 ($p=0.001$), CA IX ($p=0.001$), and GLUT-1 expression pattern ($p=0.001$). Thus, DCIS necrosis was associated with GLUT-1 positivity, CA IX positivity, and GLUT-1 central zone positivity (Figure 4).

When expression of more than two glucose metabolism-related proteins was defined as high glucose metabolism, and expression of more than three glutamine metabolism-related proteins was defined as high glutamine metabolism, high glucose metabolism was associated with ER negativity ($p=0.004$) and necrosis ($p<0.001$), and high glutamine metabolism was associated with the non-luminal subtype ($p=0.001$) and inflammatory-type stroma ($p=0.004$) (Figure 5).

Effect of metabolism-related protein expression on patient prognosis. The effect of metabolism-related protein expression on patient outcome was analyzed through univariate analysis, and the results among patients with DCIS were not significant (Supplementary Table S4).

Discussion

In this study, we evaluated glucose and glutamine metabolism-related protein expression in breast DCIS and observed differences in expression depending on the molecular subtype. Among the glucose metabolism-related proteins, the expression of hexokinase II ($p=0.044$) was more pronounced in TNBC than in other subtypes. Although

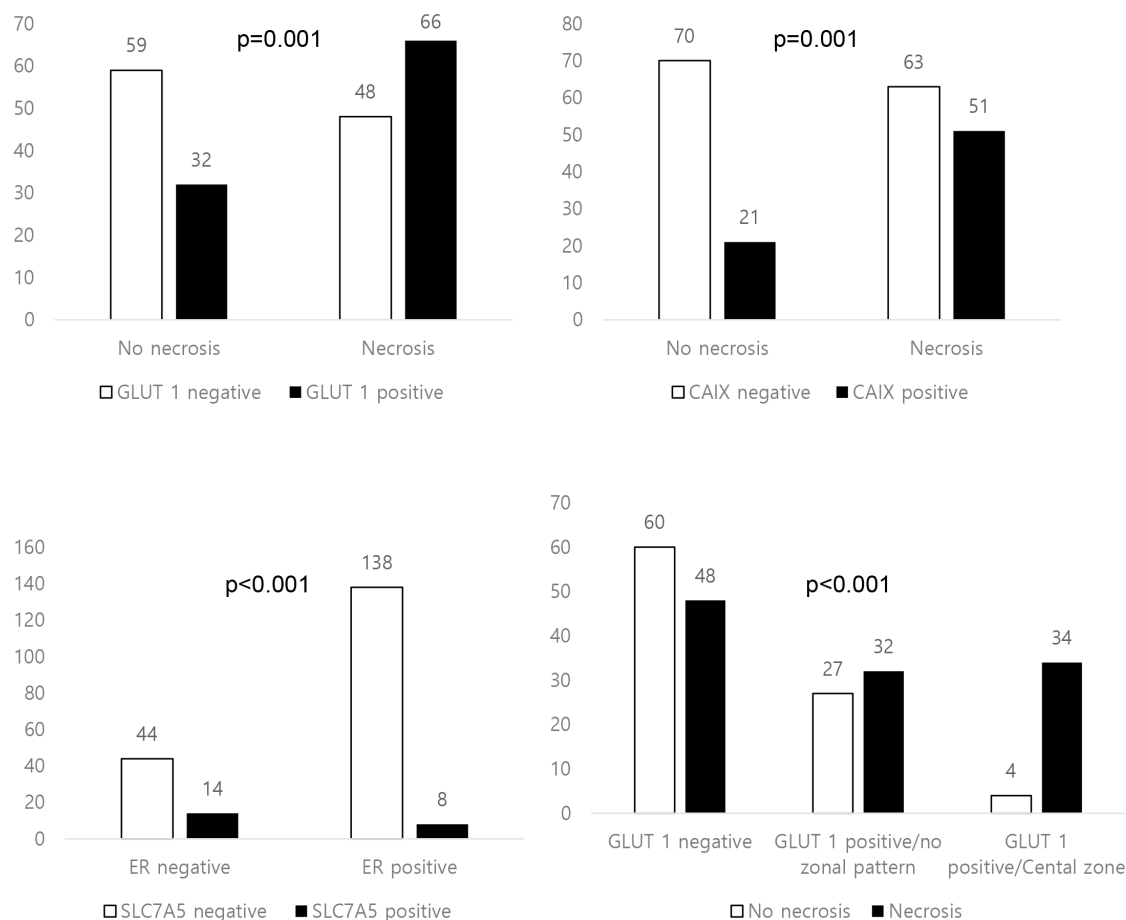


Figure 4. Correlation between the clinicopathological factors and metabolism-related protein expression. DCIS necrosis was associated with GLUT-1 positivity (p=0.001), CA IX positivity (p=0.001), and GLUT-1 central zone positivity (p=0.001).

Table 4. Glutamine metabolism-related protein expression in ductal carcinoma in situ according to stromal type.

Parameters	Total N=205 (%)	Stromal type		p-value
		Non-inflammatory n=153 (%)	Inflammatory n=52 (%)	
GLS				0.784
Negative	171 (83.4)	128 (83.7)	43 (82.7)	
Low expression	22 (10.7)	17 (11.1)	5 (9.6)	
High expression	12 (5.9)	8 (5.2)	4 (7.7)	
ASCT2				0.732
Negative	127 (62.0)	95 (62.1)	32 (61.5)	
Low expression	53 (25.9)	38 (24.8)	15 (28.8)	
High expression	25 (12.1)	20 (13.1)	5 (9.6)	
SLC7A5				< 0.001
Negative	182 (89.2)	143 (94.1)	39 (75.0)	
Low expression	12 (5.9)	4 (2.6)	8 (15.4)	
High expression	10 (4.9)	5 (3.3)	5 (9.6)	
SLC7A11				0.008
Negative	181 (88.2)	141 (92.2)	40 (76.9)	
Low expression	12 (5.9)	5 (3.3)	7 (13.5)	
High expression	12 (5.9)	7 (4.6)	5 (9.6)	

Abbreviations: GLS-glutaminase; ASCT-amino acid transporter; SLC-membrane-bound solution carrier

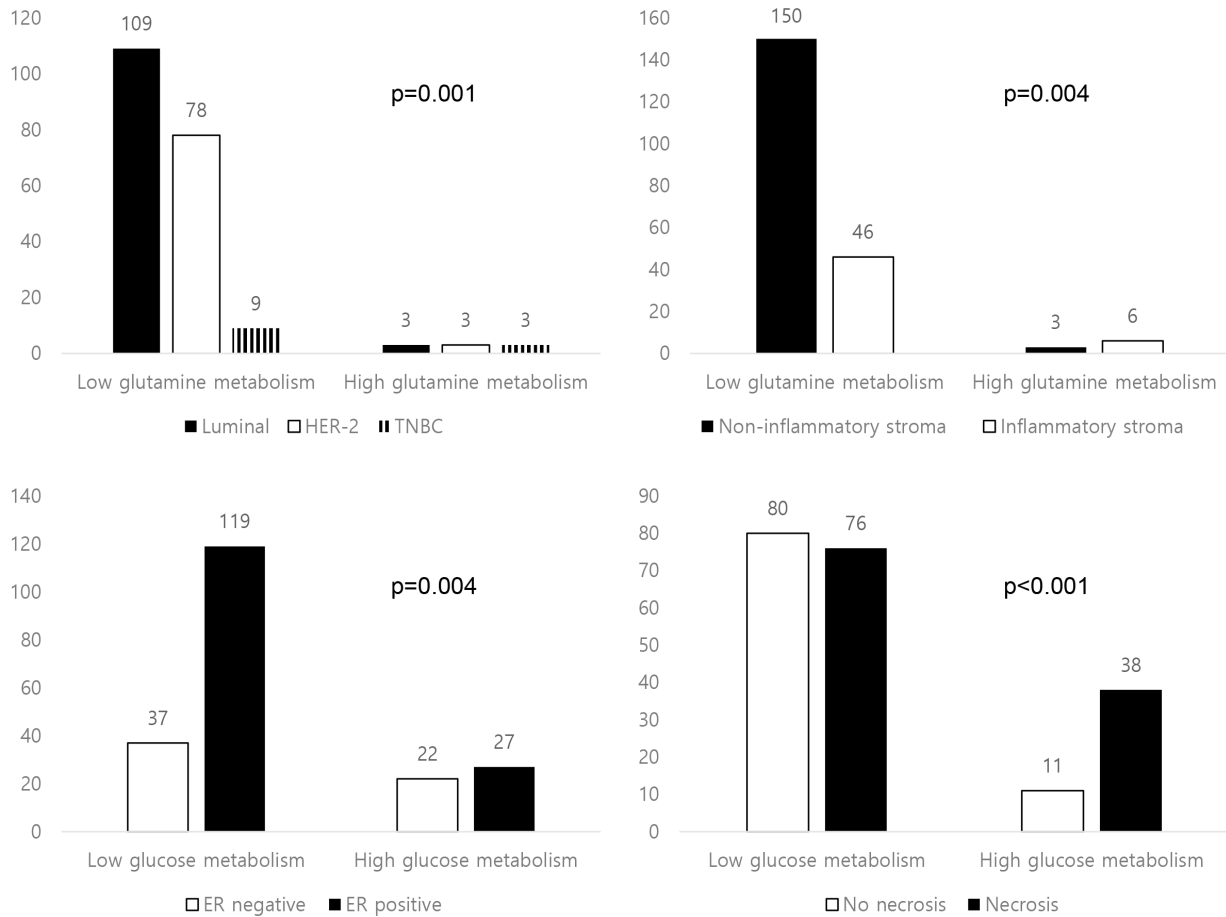


Figure 5. Correlation between the clinicopathological factors and metabolic phenotype. High glucose metabolism was associated with estrogen receptor (ER) negativity ($p=0.004$) and necrosis ($p<0.001$), and high glutamine metabolism was associated with the non-luminal subtype ($p=0.001$) and inflammatory type stoma ($p=0.004$).

no previous DCIS studies have been performed, studies on invasive breast cancer reported that glucose metabolism-related protein expression was more pronounced in TNBC than in other subtypes [26, 27], thereby supporting the findings in our study. Glucose metabolism-related proteins are highly expressed in TNBC because they may be associated with TNBC characteristics, including high metabolic activity, tumor grade, tumor necrosis, and cell proliferation [28]. The TNBC subtype of DCIS, similar to the TNBC subtype of invasive breast cancer, has been reported to be associated with high tumor grade, tumor necrosis, and cell proliferation [29], and this, in turn, suggests high metabolic activity. One of the mechanisms that enhance glucose metabolism in tumors is a hypoxic pathway through hypoxia-inducible factor (HIF)- α [30], and high cell proliferation and tumor necrosis in TNBC are likely to suggest tissue hypoxia [28]. DCIS is surrounded by a basal membrane and myoepithelial cells, and in particular, comedo-type necrosis is likely to occur in the DCIS

central zone, which is devoid of blood vessels and demonstrates tumor cell proliferation [31]. In this study, GLUT-1 expression appeared to be concentrated in the central zone, especially around the comedo-type central necrosis, in some DCIS cases, suggesting that increased cell proliferation-induced hypoxia might contribute to increased glucose metabolism in TNBC type DCIS.

In this study, among the glutamine metabolism-related proteins, GLS ($p=0.003$), which is an enzyme that converts glutamine to glutamate, and SLC7A5 ($p<0.001$) was higher in TNBC than in other subtypes. Compared to other subtypes, TNBC showed the highest ratio of glutamate to glutamine levels, suggesting the role of a deregulated glutaminolysis pathway in TNBC. This further indicated that GLS is essential for TNBC cell growth [32], thereby supporting the findings of this study. Additionally, a previous study on invasive breast cancer showed that the TNBC subtype was associated with a higher SLC7A5 expression level than the luminous subtype, demonstrating similar results to those

of our study [33]. The possible mechanisms underlying enhanced glutamine metabolism-related protein expression in TNBC involve oncogenes, such as *c-myc*, *KRAS* oncogene, and the PI3K/AKT/mTOR pathway. TNBC shows *c-myc* activation [34–36], increased *KRAS* signaling [37], and increased activity of the PI3K/AKT/mTOR pathway [38]. Further, *c-myc* combines with glutamine importers, such as ASCT-2 and SLC38A5, to promote glutamine uptake [39] and enhance GLS expression [40], and *KRAS* increases glutamine metabolism-related gene expression levels [41]. In the PI3K/AKT/mTOR pathway, mTOR complex 1 inhibits the transcription of SIRT4, an inhibitor of glutamate dehydrogenase (GDH), eventually activating GDH [42]. Next, tumor suppressors, such as Retinoblastoma protein (Rb), and glutamine metabolism may be associated. It was reported that 30% of TNBC cases showed Rb loss [43]; Rb suppresses ASCT-2 expression and reduces glutamine uptake [44]. Additionally, glutamine metabolism, similar to glucose metabolism, is associated with hypoxia, and accumulation of lactate in the tumor microenvironment during HIF-1-induced glycolysis activates *c-myc*, thereby enhancing glutaminolysis [45]. In particular, glutamine metabolism-related proteins, such as SLC7A5 ($p < 0.001$) and SLC7A11 ($p = 0.008$), were highly expressed in DCIS with inflammatory type stroma, thereby suggesting a link between glutamine metabolism and the tumor microenvironment. Interleukin (IL)-4 secreted by the immune cell increases ASCT-2 expression in breast cancer cells [46], and IL-3 increases ASCT-2 expression in the tumor microenvironment, thereby increasing glutamine uptake [47].

The clinical significance of this study is that glucose and/or glutamine metabolism inhibitors may be used for DCIS treatment and prevention. Adjuvant hormone therapy can reduce tumor recurrence in the ipsilateral breast in DCIS with ER and/or PR positive type [48, 49], but this therapy cannot be applied to DCIS without hormone receptor expression, especially the TNBC subtype. However, adjuvant therapy modality may be necessary to prevent the tumor recurrence in TNBC type DCIS, owing to its more aggressive tumor properties compared with those of hormone receptor-positive DCIS. Therefore, we suggested the use of glucose and/or glutamine metabolic inhibitors as adjuvant therapy for TNBC type DCIS. Preclinical and clinical studies have reported that hexokinase II inhibitor 3-BrPA [50], CA IX inhibitor CAN508 [51], GLS inhibitor CB-839 [52], and SLC7A5 inhibitor benzylserine [53] effectively inhibit breast cancer cell growth. However, further study is required to determine whether the administration of these drugs can inhibit the recurrence of TNBC-type DCIS.

In conclusion, metabolism-related protein expression differs according to the molecular subtype and stromal type of DCIS. Glucose and glutamine metabolism-related proteins were highly expressed in TNBC, and glutamine metabolism-related proteins were highly expressed in DCIS with inflammatory type stroma.

Supplementary information is available in the online version of the paper.

Acknowledgments: This study was approved by the Institutional Review Board of Severance Hospital (4-2020-1282). The informed consent from patients was exempted by IRB. This study was exempt from obtaining written informed consent due to the retrospective nature of the study.

References

- [1] DOEBAR SC, VAN DEN BROEK EC, KOPPERS LB, JAGER A, BAAIJENS MH et al. Extent of ductal carcinoma in situ according to breast cancer subtypes: a population-based cohort study. *Breast Cancer Res Treat* 2016; 158: 179–187. <https://doi.org/10.1007/s10549-016-3862-4>
- [2] GAO Y, NIU Y, WANG X, WEI L, LU S. Genetic changes at specific stages of breast cancer progression detected by comparative genomic hybridization. *J Mol Med (Berl)* 2009; 87: 145–152. <https://doi.org/10.1007/s00109-008-0408-1>
- [3] PAGE DL, DUPONT WD, ROGERS LW, LANDENBERGER M. Intraductal carcinoma of the breast: follow-up after biopsy only. *Cancer* 1982; 49: 751–758
- [4] SANDERS ME, SCHUYLER PA, DUPONT WD, PAGE DL. The natural history of low-grade ductal carcinoma in situ of the breast in women treated by biopsy only revealed over 30 years of long-term follow-up. *Cancer* 2005; 103: 2481–2484. <https://doi.org/10.1002/cncr.21069>
- [5] PAGE DL, DUPONT WD, ROGERS LW, JENSEN RA, SCHUYLER PA. Continued local recurrence of carcinoma 15–25 years after a diagnosis of low grade ductal carcinoma in situ of the breast treated only by biopsy. *Cancer* 1995; 76: 1197–1200. [https://doi.org/10.1002/1097-0142\(19951001\)76:7<1197::aid-cncr2820760715>3.0.co;2-0](https://doi.org/10.1002/1097-0142(19951001)76:7<1197::aid-cncr2820760715>3.0.co;2-0)
- [6] KIM JW, DANG CV. Cancer's molecular sweet tooth and the Warburg effect. *Cancer Res* 2006; 66: 8927–8930. <https://doi.org/10.1158/0008-5472.can-06-1501>
- [7] WARBURG O. On the origin of cancer cells. *Science* 1956; 123: 309–314. <https://doi.org/10.1126/science.123.3191.309>
- [8] OLSON AL, PESSIN JE. Structure, function, and regulation of the mammalian facilitative glucose transporter gene family. *Annu Rev Nutr* 1996; 16: 235–256. <https://doi.org/10.1146/annurev.nu.16.070196.001315>
- [9] LEHTO M, XIANG K, STOFFEL M, ESPINOSA R, 3RD, GROOP LC et al. Human hexokinase II: localization of the polymorphic gene to chromosome 2. *Diabetologia* 1993; 36: 1299–1302. <https://doi.org/10.1007/BF00400809>
- [10] OPAVSKY R, PASTOREKOVA S, ZELNIK V, GIBADULINOVA A, STANBRIDGE EJ et al. Human MN/CA9 gene, a novel member of the carbonic anhydrase family: structure and exon to protein domain relationships. *Genomics* 1996; 33: 480–487. <https://doi.org/10.1006/geno.1996.0223>
- [11] DEBERARDINIS RJ, CHENG T. Q's next: the diverse functions of glutamine in metabolism, cell biology and cancer. *Oncogene* 2010; 29: 313–324. <https://doi.org/10.1038/onc.2009.358>

- [12] CURTHOYS NP, WATFORD M. Regulation of glutaminase activity and glutamine metabolism. *Annu Rev Nutr* 1995; 15: 133–159. <https://doi.org/10.1146/annurev.nu.15.070195.001025>
- [13] KIM HM, KOO JS. Differential Expression of Glycolysis-Related Proteins in Follicular Neoplasms versus Hurthle Cell Neoplasms: A Retrospective Analysis. *Dis Markers* 2017; 2017: 6230294. <https://doi.org/10.1155/2017/6230294>
- [14] NAHM JH, KIM HM, KOO JS. Glycolysis-related protein expression in thyroid cancer. *Tumour Biol* 2017; 39: 1010428317695922. <https://doi.org/10.1177/1010428317695922>
- [15] SUN WY, KIM HM, JUNG WH, KOO JS. Expression of serine/glycine metabolism-related proteins is different according to the thyroid cancer subtype. *J Transl Med* 2016; 14: 168. <https://doi.org/10.1186/s12967-016-0915-8>
- [16] GOMEZ-CEBRIAN N, ROJAS-BENEDICTO A, ALBORS-VAQUER A, LOPEZ-GUERRERO JA, PINEDA-LUCENA A et al. Metabolomics Contributions to the Discovery of Prostate Cancer Biomarkers. *Metabolites* 2019; 9. <https://doi.org/10.3390/metabo9030048>
- [17] CHEN X, LU P, ZHOU S, ZHANG L, ZHAO JH et al. Predictive value of glucose transporter-1 and glucose transporter-3 for survival of cancer patients: A meta-analysis. *Oncotarget* 2017; 8: 13206–13213. <https://doi.org/10.18632/oncotarget.14570>
- [18] VAN KUIJK SJ, YAROMINA A, HOUBEN R, NIEMANS R, LAMBIN P et al. Prognostic Significance of Carbonic Anhydrase IX Expression in Cancer Patients: A Meta-Analysis. *Front Oncol* 2016; 6: 69. <https://doi.org/10.3389/fonc.2016.00069>
- [19] AVRIL N, MENZEL M, DOSE J, SCHELLING M, WEBER W et al. Glucose metabolism of breast cancer assessed by 18F-FDG PET: histologic and immunohistochemical tissue analysis. *J Nucl Med* 2001; 42: 9–16.
- [20] EL ANSARI R, MCINTYRE A, CRAZE ML, ELLIS IO, RAKHA EA et al. Altered glutamine metabolism in breast cancer; subtype dependencies and alternative adaptations. *Histopathology* 2018; 72: 183–190. <https://doi.org/10.1111/his.13334>
- [21] MAXWELL AJ, CLEMENTS K, HILTON B, DODWELL DJ, EVANS A et al. Risk factors for the development of invasive cancer in unresected ductal carcinoma in situ. *Eur J Surg Oncol* 2018; 44: 429–435. <https://doi.org/10.1016/j.ejso.2017.12.007>
- [22] ELSTON CW, ELLIS IO. Pathological prognostic factors in breast cancer. I. The value of histological grade in breast cancer: experience from a large study with long-term follow-up. *Histopathology* 1991; 19: 403–410. <https://doi.org/10.1111/j.1365-2559.1991.tb00229.x>
- [23] HAMMOND ME, HAYES DF, DOWSETT M, ALLRED DC, HAGERTY KL et al. American Society of Clinical Oncology/College of American Pathologists guideline recommendations for immunohistochemical testing of estrogen and progesterone receptors in breast cancer. *J Clin Oncol* 2010; 28: 2784–2795. <https://doi.org/10.1200/jco.2009.25.6529>
- [24] WOLFF AC, HAMMOND ME, SCHWARTZ JN, HAGERTY KL, ALLRED DC et al. American Society of Clinical Oncology/College of American Pathologists guideline recommendations for human epidermal growth factor receptor 2 testing in breast cancer. *J Clin Oncol* 2007; 25: 118–145. <https://doi.org/10.1200/jco.2006.09.2775>
- [25] GOLDHIRSCH A, WOOD WC, COATES AS, GELBER RD, THURLIMANN B et al. Strategies for subtypes--dealing with the diversity of breast cancer: highlights of the St. Gallen International Expert Consensus on the Primary Therapy of Early Breast Cancer 2011. *Ann Oncol* 2011; 22: 1736–1747. <https://doi.org/10.1093/annonc/mdr304>
- [26] CHOI J, JUNG WH, KOO JS. Metabolism-related proteins are differentially expressed according to the molecular subtype of invasive breast cancer defined by surrogate immunohistochemistry. *Pathobiology* 2013; 80: 41–52. <https://doi.org/10.1159/000339513>
- [27] TAN EY, YAN M, CAMPO L, HAN C, TAKANO E et al. The key hypoxia regulated gene CAIX is upregulated in basal-like breast tumours and is associated with resistance to chemotherapy. *Br J Cancer* 2009; 100: 405–411. <https://doi.org/10.1038/sj.bjc.6604844>
- [28] BIANCHINI G, BALKO JM, MAYER IA, SANDERS ME, GIANNI L. Triple-negative breast cancer: challenges and opportunities of a heterogeneous disease. *Nat Rev Clin Oncol* 2016; 13: 674–690. <https://doi.org/10.1038/nrclinonc.2016.66>
- [29] VANDENBUSSCHE CJ, ELWOOD H, CIMINOMATHEWS A, BITTAR Z, ILLEI PB et al. Clinicopathologic features of ductal carcinoma in situ in young women with an emphasis on molecular subtype. *Hum Pathol* 2013; 44: 2487–2493. <https://doi.org/10.1016/j.humpath.2013.06.007>
- [30] SEMENZA GL. Hypoxia-inducible factors: coupling glucose metabolism and redox regulation with induction of the breast cancer stem cell phenotype. *EMBO J* 2017; 36: 252–259. <https://doi.org/10.15252/embj.201695204>
- [31] BUSSOLATI G, BONGIOVANNI M, CASSONI P, SAPINO A. Assessment of necrosis and hypoxia in ductal carcinoma in situ of the breast: basis for a new classification. *Virchows Arch* 2000; 437: 360–364. <https://doi.org/10.1007/s004280000267>
- [32] LAMPA M, ARLT H, HE T, OSPINA B, REEVES J et al. Glutaminase is essential for the growth of triple-negative breast cancer cells with a deregulated glutamine metabolism pathway and its suppression synergizes with mTOR inhibition. *PLoS One* 2017; 12: e0185092. <https://doi.org/10.1371/journal.pone.0185092>
- [33] FURUYA M, HORIGUCHI J, NAKAJIMA H, KANAI Y, OYAMA T. Correlation of L-type amino acid transporter 1 and CD98 expression with triple negative breast cancer prognosis. *Cancer Sci* 2012; 103: 382–389. <https://doi.org/10.1111/j.1349-7006.2011.02151.x>
- [34] CHANDRIANI S, FRENGEN E, COWLING VH, PENDERGRASS SA, PEROU CM et al. A core MYC gene expression signature is prominent in basal-like breast cancer but only partially overlaps the core serum response. *PLoS One* 2009; 4: e6693. <https://doi.org/10.1371/journal.pone.0006693>

- [35] HORIUCHI D, KUSDRA L, HUSKEY NE, CHANDRIANI S, LENBURG ME et al. MYC pathway activation in triple-negative breast cancer is synthetic lethal with CDK inhibition. *J Exp Med* 2012; 209: 679–696. <https://doi.org/10.1084/jem.20111512>
- [36] KATSUTA E, YAN L, TAKESHITA T, MCDONALD KA, DASGUPTA S et al. High MYC mRNA Expression Is More Clinically Relevant than MYC DNA Amplification in Triple-Negative Breast Cancer. *Int J Mol Sci* 2019; 21. <https://doi.org/10.3390/ijms21010217>
- [37] TOKUMARU Y, OSHI M, KATSUTA E, YAN L, SATYANANDA V et al. KRAS signaling enriched triple negative breast cancer is associated with favorable tumor immune microenvironment and better survival. *Am J Cancer Res* 2020; 10: 897–907.
- [38] COSSU-ROCCA P, ORRÛ S, MURONI MR, SANGES F, SOTGIU G et al. Analysis of PIK3CA Mutations and Activation Pathways in Triple Negative Breast Cancer. *PLoS One* 2015; 10: e0141763. <https://doi.org/10.1371/journal.pone.0141763>
- [39] WISE DR, DEBERARDINIS RJ, MANCUSO A, SAYED N, ZHANG XY et al. Myc regulates a transcriptional program that stimulates mitochondrial glutaminolysis and leads to glutamine addiction. *Proc Natl Acad Sci U S A* 2008; 105: 18782–18787. <https://doi.org/10.1073/pnas.0810199105>
- [40] GAO P, TCHERNYSHYOV I, CHANG TC, LEE YS, KITA K et al. c-Myc suppression of miR-23a/b enhances mitochondrial glutaminase expression and glutamine metabolism. *Nature* 2009; 458: 762–765. <https://doi.org/10.1038/nature07823>
- [41] GAGLIO D, METALLO CM, GAMEIRO PA, HILLER K, DANNA LS et al. Oncogenic K-Ras decouples glucose and glutamine metabolism to support cancer cell growth. *Mol Syst Biol* 2011; 7: 523. <https://doi.org/10.1038/msb.2011.56>
- [42] CSIBI A, FENDT SM, LI C, POULOGIANNIS G, CHOO AY et al. The mTORC1 pathway stimulates glutamine metabolism and cell proliferation by repressing SIRT4. *Cell* 2013; 153: 840–854. <https://doi.org/10.1016/j.cell.2013.04.023>
- [43] WITKIEWICZ AK, KNUDSEN ES. Retinoblastoma tumor suppressor pathway in breast cancer: prognosis, precision medicine, and therapeutic interventions. *Breast Cancer Res* 2014; 16: 207. <https://doi.org/10.1186/bcr3652>
- [44] REYNOLDS MR, LANE AN, ROBERTSON B, KEMP S, LIU Y et al. Control of glutamine metabolism by the tumor suppressor Rb. *Oncogene* 2014; 33: 556–566. <https://doi.org/10.1038/onc.2012.635>
- [45] PÉREZ-ESCUREDO J, DADHICH RK, DHUP S, CACACE A, VAN HËE VF et al. Lactate promotes glutamine uptake and metabolism in oxidative cancer cells. *Cell Cycle* 2016; 15: 72–83. <https://doi.org/10.1080/15384101.2015.1120930>
- [46] VENMAR KT, KIMMEL DW, CLIFFEL DE, FINGLETON B. IL4 receptor α mediates enhanced glucose and glutamine metabolism to support breast cancer growth. *Biochim Biophys Acta* 2015; 1853: 1219–1228. <https://doi.org/10.1016/j.bbamcr.2015.02.020>
- [47] WELLEN KE, LU C, MANCUSO A, LEMONS JM, RYCKZO M et al. The hexosamine biosynthetic pathway couples growth factor-induced glutamine uptake to glucose metabolism. *Genes Dev* 2010; 24: 2784–2799. <https://doi.org/10.1101/gad.1985910>
- [48] CUZICK J, SESTAK I, PINDER SE, ELLIS IO, FORSYTH S et al. Effect of tamoxifen and radiotherapy in women with locally excised ductal carcinoma in situ: long-term results from the UK/ANZ DCIS trial. *Lancet Oncol* 2011; 12: 21–29. [https://doi.org/10.1016/s1470-2045\(10\)70266-7](https://doi.org/10.1016/s1470-2045(10)70266-7)
- [49] THOMPSON AM, CLEMENTS K, CHEUNG S, PINDER SE, LAWRENCE G et al. Management and 5-year outcomes in 9938 women with screen-detected ductal carcinoma in situ: the UK Sloane Project. *Eur J Cancer* 2018; 101: 210–219. <https://doi.org/10.1016/j.ejca.2018.06.027>
- [50] ZHANG Q, ZHANG Y, ZHANG P, CHAO Z, XIA F et al. Hexokinase II inhibitor, 3-BrPA induced autophagy by stimulating ROS formation in human breast cancer cells. *Genes Cancer* 2014; 5: 100–112. <https://doi.org/10.18632/gene-sandcancer.9>
- [51] SAID MA, ELDEHNA WM, NOCENTINI A, FAHIM SH, BONARDI A et al. Sulfonamide-based ring-fused analogues for CAN508 as novel carbonic anhydrase inhibitors endowed with antitumor activity: Design, synthesis, and in vitro biological evaluation. *Eur J Med Chem* 2020; 189: 112019. <https://doi.org/10.1016/j.ejmech.2019.112019>
- [52] GROSS MI, DEMO SD, DENNISON JB, CHEN L, CHERNOV-ROGAN T et al. Antitumor activity of the glutaminase inhibitor CB-839 in triple-negative breast cancer. *Mol Cancer Ther* 2014; 13: 890–901. <https://doi.org/10.1158/1535-7163.Mct-13-0870>
- [53] VAN GELDERMALSEN M, QUEK LE, TURNER N, FREDMAN N, PANG A et al. Benzylserine inhibits breast cancer cell growth by disrupting intracellular amino acid homeostasis and triggering amino acid response pathways. *BMC Cancer* 2018; 18: 689. <https://doi.org/10.1186/s12885-018-4599-8>

https://doi.org/10.4149/neo_2022_220103N3

Glucose and glutamine metabolism-related protein expression in breast ductal carcinoma *in situ*

Hyang Joo RYU, Ja Seung KOO*

Supplementary Information

Supplementary Table S1. Source, clone, and dilution of antibodies.

Antibody	Company	Clone	Dilution
Glucose metabolism related proteins			
GLUT 1	Abcam, Cambridge, UK	SPM498	1:200
Hexokinase II	Abcam, Cambridge, UK	3D3	1:200
CA IX	Abcam, Cambridge, UK	Polyclonal	1:500
Glutamine metabolism related proteins			
GLS	Abcam, Cambridge, UK	EP7212	1:100
ASCT2	Invitrogen	Polyclonal	1:50
SLC7A5	Abcam, Cambridge, UK	EPR17573	1:500
SLC7A11	Abcam, Cambridge, UK	Polyclonal	1:200
Molecular subtype related proteins			
ER	Thermo Scientific, San Diego, CA, USA	SP1	1:100
PR	DAKO, Glostrup, Denmark	PgR	1:50
HER-2	DAKO, Glostrup, Denmark	Polyclonal	1:1500
Ki-67	Abcam, Cambridge, UK	MIB	1:1000

Supplementary Table S2. Basal characteristics of ductal carcinoma *in situ*.

Parameters	Total N=205 (%)	Molecular subtype			p-value
		Luminal n=112 (%)	HER-2 n=81 (%)	TNBC n=12 (%)	
Age (years)					0.047
≤50	118 (57.6)	73 (65.2)	40 (49.4)	5 (41.7)	
>50	87 (42.4)	39 (34.8)	41 (50.6)	7 (58.3)	
Architecture type					0.002
Cribriform	92 (44.9)	64 (57.1)	26 (32.1)	2 (16.7)	
Solid	82 (40.0)	36 (32.1)	38 (49.6)	8 (66.7)	
Micropapillary	20 (9.8)	6 (5.4)	12 (14.8)	2 (16.7)	
Papillary	8 (3.9)	6 (5.4)	2 (2.5)	0 (0.0)	
Apocrine	3 (1.5)	0 (0.0)	3 (3.7)	0 (0.0)	
Nuclear grade					0.002
Low	13 (6.3)	9 (8.0)	4 (4.9)	0 (0.0)	
Intermediate	109 (52.3)	67 (59.8)	41 (50.6)	1 (8.3)	
High	83 (40.5)	36 (32.1)	36 (44.4)	11 (91.7)	
Necrosis					<0.001
Absent	91 (44.4)	66 (58.9)	20 (24.7)	5 (41.7)	
Focal	33 (16.1)	21 (18.8)	11 (13.6)	1 (8.3)	
Comedo	81 (39.5)	25 (22.3)	50 (61.7)	6 (50.0)	
Stromal type					<0.001
Non-inflammatory	153	102	45	6	
Inflammatory	52 (25.4)	10 (8.9)	36 (44.4)	6 (50.0)	

Supplementary Table S3. Expression of GLS and SLC7A5 according to the hexokinase II expression status in ductal carcinoma *in situ*.

Parameters	Total N=205 (%)	Hexokinase II		p-value
		Negative n=188 (%)	Positive n=17 (%)	
GLS				0.902
Negative	171 (83.4)	157 (83.5)	14 (82.4)	
Positive	34 (16.6)	31 (16.5)	3 (17.6)	
SLC7A5				0.336
Negative	183 (89.3)	169 (89.9)	14 (82.4)	
Positive	22 (10.7)	19 (10.1)	3 (17)	

Supplementary Table S4. Univariate analysis of the impact of metabolism-related proteins expression on DCIS prognosis by Log-rank analysis.

Parameter	Disease-free survival		Overall survival	
	Mean survival (95% CI) months	p-value	Mean survival (95% CI) months	p-value
Hexokinase II		n/a		n/a
Negative	188/4/3	n/a	n/a	
Positive	17/0/0	n/a	n/a	
GLUT 1		0.380		0.509
Negative	107/3/1	144 (142–147)	145 (143–147)	
Positive	98/1/2	145 (144–146)	144 (141–146)	
CA IX		0.712		
Negative	133/3/2	145 (143–147)	145 (143–147)	
Positive	72/1/1	144 (142–147)	144 (142–147)	
GLS		0.599		
Negative	171/3/2	145 (143–147)	145 (144–147)	
Positive	34/1/1	144 (140–147)	143 (138–148)	
ASCT2		0.838		0.879
Negative	127/3/2	145 (143–147)	145 (143–147)	
Positive	78/1/1	143 (141–144)	142 (139–145)	
SLC7A5		n/a		n/a
Negative	183/4/3	n/a	n/a	
Positive	22/0/0	n/a	n/a	
SLC7A11		n/a		0.249
Negative	181/4/2	n/a	145 (144–147)	
Positive	4/0/1	n/a	142 (135–149)	